THE JOURNAL OF BIOLOGICAL CHEMISTRY VOL. 287, NO. 49, pp. 41560–41568, November 30, 2012

Fluorescence Resonance Energy Transfer (FRET) Indicates That Association with the Type I Ryanodine Receptor (RyR1) Causes Reorientation of Multiple Cytoplasmic Domains of the Dihydropyridine Receptor (DHPR) α_{1S} Subunit*

Received for publication, July 24, 2012, and in revised form, October 10, 2012 Published, JBC Papers in Press, October 15, 2012, DOI 10.1074/jbc.M112.404194

Alexander Polster[‡§], **Joshua D. Ohrtman**[§], **Kurt G. Beam**[§], **and Symeon Papadopoulos**[‡1]

From the [‡]*Department of Vegetative Physiology, University of Cologne, D-50931 Cologne, Germany and* [§]*Department of Physiology and Biophysics, University of Colorado Anschutz Medical Campus, Aurora, Colorado 80045*

Background: In skeletal muscle, DHPR cytoplasmic domains are thought to couple membrane depolarization to Ca^{2+} release via RyR1.
Results: The presence of RyR1 alters FRET between donor/acceptor pairs in cytoplasmic domains of the DHPR α_{1S} subunit.
Conclusion: Interaction with RyR1 causes rearrangement of α_{1S} cytoplasmic domains.
Significance: Multiple cytoplasmic domains of α_{1S} may be involved in the interaction with RyR1.

The skeletal muscle dihydropyridine receptor (DHPR) in the t-tubular membrane serves as the Ca^{2+} channel and voltage sensor for excitation-contraction (EC) coupling, triggering Ca^{2+} release via the type 1 ryanodine receptor (RyR1) in the sarcoplasmic reticulum (SR). The two proteins appear to be physically linked, and both the α_{1S} and β_{1a} subunits of the DHPR are essential for EC coupling. Within α_{1S}, cytoplasmic domains of importance include the I-II loop (to which β_{1a} binds), the II-III and III-IV loops, and the C terminus. However, the spatial relationship of these domains to one another has not been established. Here, we have taken the approach of measuring FRET between fluorescent proteins inserted into pairs of α_{1S} cytoplasmic domains. Expression of these constructs in dyspedic (RyR1 null) and dysgenic (α_{1S} null) myotubes was used to test for function and targeting to plasma membrane/SR junctions and to test whether the presence of RyR1 caused altered FRET. We found that in the absence of RyR1, measureable FRET occurred between the N terminus and C terminus (residue 1636), and between the II-III loop (residue 626) and both the N and C termini; the I-II loop (residue 406) showed weak FRET with the II-III loop but not with the N terminus. Association with RyR1 caused II-III loop FRET to decrease with the C terminus and increase with the N terminus and caused I-II loop FRET to increase with both the II-III loop and N terminus. Overall, RyR1 appears to cause a substantial reorientation of the cytoplasmic α_{1S} domains consistent with their becoming more closely packed.

In skeletal muscle, excitation-contraction (EC)[2] coupling depends upon junctions between the plasma membrane and sarcoplasmic reticulum (SR) (1). At these junctions, dihydropyridine receptors (DHPRs), which are heteromeric proteins, serve as voltage sensors that respond to depolarization by triggering the release of Ca^{2+} from the SR via the type 1 ryanodine receptor (RyR1), a homotetrameric protein (2–4). In the junctional membrane, DHPRs are arrayed in groups of four ("tetrads") as a consequence of physical links with RyR1 (5, 6). The existence of these links and the fact that skeletal-type EC coupling does not require the entry of external Ca^{2+} have led to the idea that conformational changes of the linking regions are responsible for the activation of RyR1 (7, 8). However, the identity of the linking regions has remained obscure in large measure because the interaction takes place between two separate membrane systems and depends upon voltage across the plasma membrane.

A variety of approaches has been used to try to identify the sites of linkage between the DHPR and RyR1, including binding assays *in vitro* and functional analysis of muscle cells after expression of proteins having altered sequence in specific regions. In the case of RyR1, this approach has shown that skeletal-type EC coupling depends on multiple regions far separated in the primary sequence (9, 10). However, these studies have been hampered by the relative lack of information about the tertiary structure of RyR1. There has been somewhat more progress for the DHPR because of its smaller size and its better understood domain structure. The principle subunit, α_{1S}, has four homology repeats, which form the voltage-sensing and ion permeation structures. The N and C termini and the loops linking the repeats are all cytoplasmic (11). Two loops of particular importance are the I-II loop, which is known to bind the auxiliary β_{1a} subunit (12), and the II-III loop, which is critical for both tetrad formation (13) and skeletal-type EC coupling (14–17). The β_{1a} subunit is a soluble protein which binds to α_{1S} and promotes its membrane trafficking (18). Moreover, β_{1a} is coequal in importance with the α_{1S} II-III loop for tetrad formation (19) and skeletal EC coupling (20, 21). Among the possible explanations for these results is that β_{1a} and/or the II-III loop bind to RyR1, perhaps in close proximity to one another. There

* This work was supported by Deutsche Forschungsgemeinschaft Grant PA 801/6-1 (to S. P.) and by National Institutes of Health Grants AR055104 and MDA 176448 (to K. G. B.).
[1] To whom correspondence should be addressed: Dept. of Vegetative Physiology, University of Cologne, Robert-Koch-Str. 39, D-50931 Cologne, Germany. Tel.: 49-221-478-6948; Fax: 49-221-478-3538; E-mail: spapadop@uni-koeln.de.
[2] The abbreviations used are: EC, excitation-contraction; DHPR, dihydropyridine receptor; RyR1, type 1 ryanodine receptor; SR, sarcoplasmic reticulum; AID, α_{1S} interaction domain.

is also evidence suggestive of binding interactions between other DHPR cytoplasmic domains and RyR1. These include the α_{1S} III-IV loop, which is known to modulate EC coupling (22, 23), and the C terminus, a segment of which binds to RyR1 *in vitro* (24), and which becomes partially occluded in the presence of RyR1 *in vivo* (25, 26).

The evidence that multiple cytoplasmic domains of the DHPR may interact with RyR1 makes it important to determine the spatial interrelationships between these cytoplasmic domains within living muscle cells and whether these interrelationships are altered by the presence of RyR1. In the current study, we have investigated this issue by constructing cDNAs encoding α_{1S} subunits doubly tagged with fluorescent proteins, in which a FRET donor (CyPet) was placed at one cytoplasmic site and a FRET acceptor (YPet) was situated at a second site. These constructs were expressed in skeletal myotubes produced from dyspedic (RyR1 null) and dysgenic (α_{1S} null) mice. After expression in dyspedic myotubes, energy transfer indicated proximity (<10 nm separation) between N- and C termini and between the II-III loop and both termini. By contrast, the I-II loop produced weak FRET with the II-III loop and none with the N or C termini. After expression in dysgenic myotubes, the presence of RyR1 appeared to cause a substantial reorientation of the domains, including a shift of the II-III loop toward the C terminus and a shift of the I-II loop toward both the II-III loop and N terminus. Because the I-II loop is associated with β_{1a}, the decreased proximity between the I-II and II-III loops may indicate that β_{1a} and the II-III loop form a unified structure that interacts with RyR1 to promote tetrad formation and skeletal-type EC coupling.

EXPERIMENTAL PROCEDURES

DNA Constructs for the Expression of Fluorescently Labeled α_{1S}—The backbone of the mammalian expression vectors pECFP and pEYFP (Clontech, Palo Alto, CA) was used to design plasmids for expression of fluorescently tagged rabbit α_{1S} (GenBank™ accession no. M23919). Site-directed mutagenesis (Stratagene, La Jolla, CA) was used to generate unique restriction sites at defined positions within the α_{1S} cDNA sequence, which were used to introduce the sequences encoding the FRET-optimized fluorescent proteins CyPet and/or YPet (27). The labeling positions were as follows.

CyPet-α_{1S}-YPet and YPet-α_{1S}-CyPet—One fluorescent protein was attached to the first residue of the α_{1S} N terminus, separated by the 12-residue linker RSRAQASNSAVD. The second fluorescent protein was attached to the last residue of α_{1S} truncated at residue 1636, separated by the four-residue linker PVAT.

CyPet or YPet within the α_{1S} I-II Loop—The fluorescent protein was inserted with its N terminus immediately after residue 406 of the α_{1S} I-II loop, and its C terminus connected via the 3-residue linker RLN to α_{1S} residues 407–1860.

CyPet or YPet within the α_{1S} II-III Loop—The fluorescent protein sequence was inserted into the II-III loop between α_{1S} residues 726 and 727, connected via a four-residue linker (PVAT) and 18-residue linker (RSRAQASNSAVDGTAGPV), respectively.

CyPet or YPet within the α_{1S} III-IV Loop—The fluorescent protein sequence was inserted into the III-IV loop between α_{1S} residues 1096 and 1097 via a single leucine and a three-residue linker (SAR), respectively.

YPet-α_{1S}-α_{1S}-CyPet (α_{1S} tandem)—The first α_{1S} was attached via its C terminus, which had been truncated at residue 1636, to a three-residue linker (GVD), which was attached to the N terminus of the second α_{1S}, which was C-terminally truncated at residue 1636. YPet was attached to the N terminus of the first α_{1S} via a 12-residue linker (SRAQASNSAVD) and CyPet was attached to the C terminus of the second α_{1S} via a four-residue linker (PVAT).

Primary Skeletal Muscle Cell Culture and Transfection—Myoblasts were prepared from newborn dysgenic mice, homozygous for absence of α_{1S} (28), or newborn dyspedic mice, homozygous for absence of RyR1 (29) as described (30). The myoblasts were grown for 6–7 days in a humidified 37 °C incubator with 5% CO_2 in Dulbecco's modified eagle medium (E15-009, PAA, Coelbe, Germany), supplemented with 10% fetal bovine serum/10% horse serum (Biochrom, Berlin, Germany). This medium was then replaced with differentiation medium (DMEM supplemented with 2% horse serum). Two to four days following the shift to differentiation medium, single nuclei were microinjected with plasmid cDNA (100 ng/μl in water).

Microscopy and Measurements of FRET—An important consideration for the studies reported here is that fluorescently tagged α_{1S} constructs expressed in myotubes are concentrated in numerous discrete foci of small size ($\leq$1 μm). Thus, methods for analysis of FRET, which require multiple scans, have the drawback that the measurements will be compromised if movement of the foci occurs in the time interval between the initial and final scans, an interval that can be substantial. For example, the acceptor photobleaching method requires the measurement of cyan fluorescence before after the bleaching of yellow and typically requires several seconds or more. Thus, we selected to employ a method in which an index of FRET could be obtained without multiple scans. Specifically, myotubes were examined 24–48 h after microinjection using a FV1000 confocal laser-scanning microscope (Olympus) under 60× magnification. For the measurement of FRET, an area of 512 × 512 pixels was selected to include both a part of the myotube to be analyzed and an adjacent region, which was cell-free. Excitation was at 440 nm, and emission was measured simultaneously via two photomultipliers, one of which was equipped with a 465–495 nm band pass filter (*cyan channel*, intensity I_C), and the other photomultiplier was equipped with a 535–565 nm band pass filter (*yellow channel*, intensity I_Y). The photomultiplier gains, offsets, and pinhole diameters were kept the same for all experiments. Even when both YPet and CyPet are present, only CyPet contributes to I_C because YPet does not emit in the 465–495 nm range. However, I_Y contains three contributions, emission from CyPet in the 535–565 nm range ($I_{Y(Cy)}$), emission from YPet, which is directly excited by 440 nm ($I_{Y(Y)}$), and YPet emission, which occurs as a consequence of FRET ($I_{Y(FRET)}$).

$$I_Y = I_{Y(Cy)} + I_{Y(Y)} + I_{Y(FRET)} \quad \text{(Eq. 1)}$$

Correction for $I_{Y(Cy)}$ is straightforward because the magnitude of $I_{Y(Cy)}$ is a constant fraction of I_C. To determine this fraction, we measured I_C and $I_{Y(Cy)}$ in cells expressing α_{1S} labeled only with a single CyPet and excited at 440 nm. This yielded $I_{Y(Cy)}/I_C = 0.28 \pm 0.02$ ($n = 25$). Thus, for constructs labeled with both CyPet and YPet, we calculated the following in Equation 2.

$$I_Y^* = I_{Y(Y)} + I_{Y(FRET)} - 0.28 \cdot I_C \quad \text{(Eq. 2)}$$

In principle, it would also have been possible to have corrected for $I_{Y(Y)}$ (emission from YPet excited at 440 nm) by scanning each cell twice, once with 440 nm excitation and once with 515 nm excitation (which does not excite CyPet). However, because 440 nm is near the absorption minimum for YPet, we chose for simplicity to calculate Equation 3 as an indication of FRET.

$$I_Y^*/I_C \quad \text{(Eq. 3)}$$

The calculation of I_Y^*/I_C was restricted to the punctate foci to which labeled α_{1S} constructs localize in myotubes. First, the background intensity measured in a cell-free region was subtracted from all pixels of the respective scan. Then, by means of a custom made Microsoft Excel macro, the image was "masked" with an adjustable threshold, such that all areas below this threshold were excluded from analysis, and only areas exceeding the threshold (including the punctate foci) were included. The macro iteratively incremented the cut-off intensity, resulting in a successively decreasing number of included pixels. For each value of the threshold, the macro calculated $I_Y^* = I_Y - 0.28 \cdot I_C$ and the ratio I_Y^*/I_C. During this iterative process, I_Y^*/I_C approached a quasi-constant level as the threshold was increased and the contribution of regions outside the punctate foci was reduced. Subsequently, I_Y^*/I_C abruptly became unstable when the cut-off threshold became so high that the small size of the analyzed areas caused large inhomogeneities in pixel levels between the cyan and yellow channels. The values of I_Y^*/I_C reported under "Results" (see Figs. 3 and 4) are from the approximately constant-level phase as revealed by the analysis macro. All data are reported as mean ± S.D. The unpaired Student's *t* test was used to compare the I_Y^*/I_C ratios calculated for a given construct expressed in dyspedic or dysgenic myotubes.

Electrically Evoked Contractions—The ability of fluorescently labeled α_{1S} constructs to support EC coupling was tested by determining whether myotubes expressing the construct and bathed in rodent Ringer's (146 mM NaCl, 5 mM KCl, 2 mM $CaCl_2$, 1 mM $MgCl_2$, 10 mM HEPES, 11 mM glucose, pH 7.40, with NaOH) contracted in response to a 10-ms, 100-V pulse applied via an extracellular pipette filled with 150 mM NaCl.

Measurement of L-type Currents—The whole cell patch clamp method was used to measure macroscopic Ca^{2+} currents (31). Borosilicate glass pipettes were polished to a final resistance of ~2.0–3.0 MΩ when filled with intracellular solution containing the following: 140 mM CsAsp, 5 mM $MgCl_2$, 10 mM Cs_2EGTA, 10 mM HEPES, pH 7.4, with CsOH. The external bath solution contained the following: 10 mM $CaCl_2$, 145 mM tetraethylammonium-Cl, 0.003 mM tetrodotoxin, 0.1 mM *N*-benzyl-*p*-toluene sulfonamide, 10 mM HEPES, pH 7.4 with tetraethylammonium-OH. To isolate L-type currents, voltage was stepped from the holding potential (−80 mV) to −20 mV for 1 s to inactivate endogenous T-type current and then repolarized to −50 mV for 50 ms, depolarized to varying test potentials for 200–400 ms, repolarized to −50 mV for 100 ms, and then returned to the holding potential. Test currents were corrected for linear components of leak and capacitive current by digitally scaling and subtracting the average of 11 control currents elicited by a hyperpolarizing step from −80 to −110 mV. Cell capacitance was determined by integration of a transient from −80 to −70 mV and was used to normalize current amplitudes (pA/pF). Peak currents as a function of test potential were fitted according to Equation 4,

$$I = G_{max} \cdot (V - V_{rev})/\{1 + \exp[-(V - V_{1/2})/k_G]\} \quad \text{(Eq. 4)}$$

where I is the peak inward Ca^{2+} current measured at the potential V, V_{rev} is the reversal potential, and k_G is a slope factor.

RESULTS

Sites within α_{1S} Cytoplasmic Domains Suitable for Labeling with Fluorescent Protein—The goal of this study was to determine whether association with RyR1 causes rearrangement of the cytoplasmic domains of α_{1S}, as indicated by altered FRET between donor/acceptor pairs inserted at various cytoplasmic sites. A necessary requirement for these constructs was that they target to plasma membrane/SR junctions in both dyspedic (RyR1 null) and dysgenic (α_{1S} null) myotubes and that they function as both L-type Ca^{2+} channels and voltage sensors for EC coupling after expression in dysgenic myotubes. Correct targeting was assessed by the presence of discrete, fluorescent foci (~0.3–1 μm in diameter) located close to or at the cell surface. Focal extracellular stimulation was used to test for contractions as an indicator of EC coupling, and whole-cell voltage clamp measurements were used to test for L-type Ca^{2+} current.

As a first step toward double labeling α_{1S} with fluorescent proteins, we tested constructs with single additions to the cytoplasmic domains. As expected from previous work (25), a construct in which the fluorescent protein was attached to the N terminus, produced fluorescent puncta in both dyspedic and dysgenic myotubes, and was able to produce L-type Ca^{2+} current and support EC coupling in dysgenic myotubes (Fig. 1*a*). The effects of insertion into the I-II loop depended on whether this was upstream or downstream of the AID (residues 357–374), at which high affinity binding of β_{1a} occurs (32). A construct with upstream insertion (between residues 350 and 351) failed to target in dyspedic myotubes and did not restore Ca^{2+} channel and EC coupling functions in dysgenic myotubes, although targeting in dysgenic myotubes still appeared to occur (Fig. 1*b*). Insertion downstream of the AID, between residues 406 and 407, did not interfere with either targeting or function (Fig. 1*c*). Previous work (33) had shown targeting to be unaffected, and function to be only partially reduced, after expression in dysgenic myotubes of a construct in which a single fluorescent protein had been inserted into the II-III loop between residues 726 and 727, which is near the N terminus of a domain (residues 720–765) known to be critical for EC coupling (16). Here, we also found that targeting and function in dysgenic myotubes were preserved after insertion of fluorescent protein

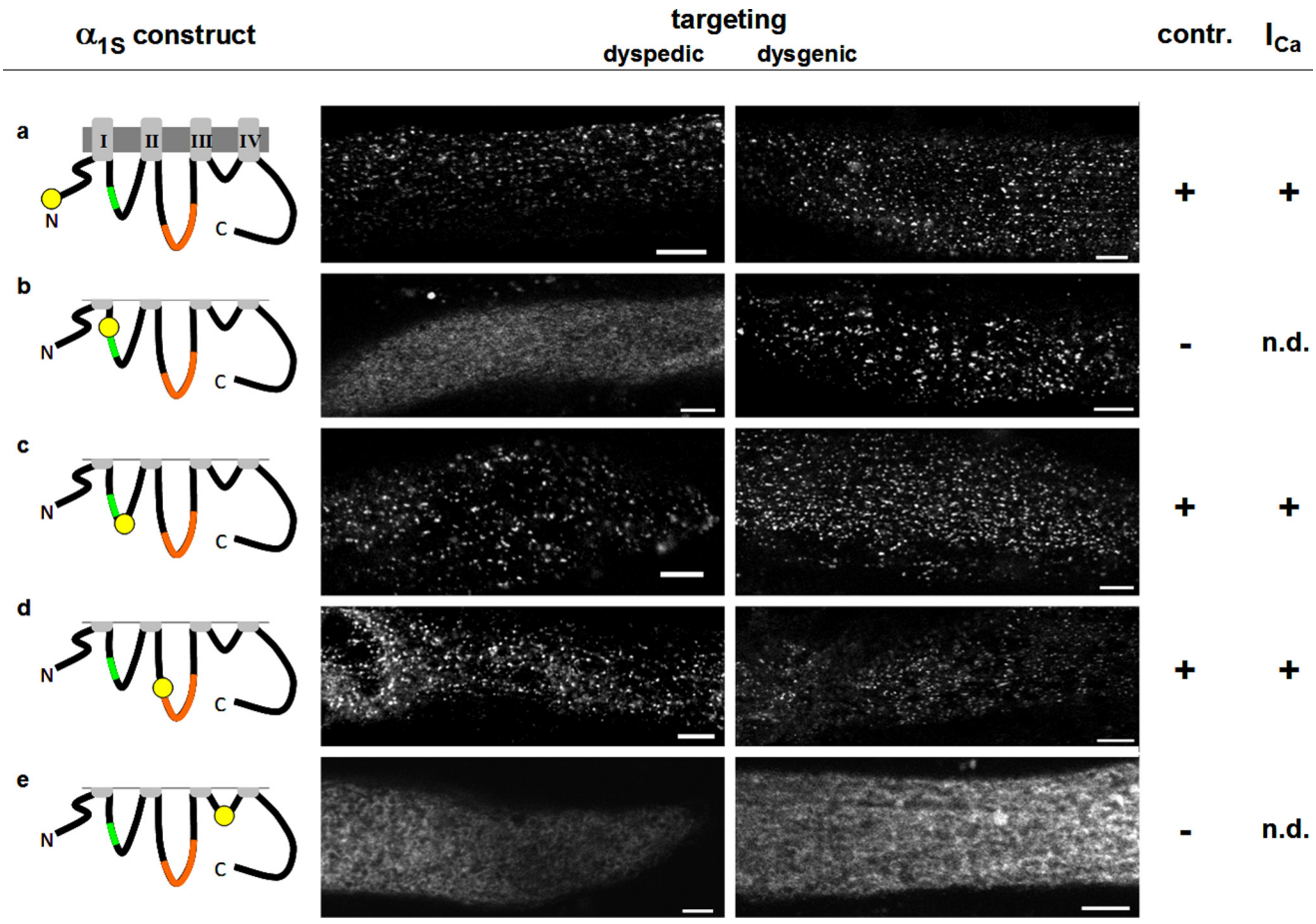

FIGURE 1. **Positions within α_{1S} cytoplasmic domains suitable for labeling with fluorescent protein.** The *schematics* on the *left* indicate the cytoplasmic α_{1S} regions that were tagged with YPet. The *Roman numerals* indicate the four homologous α_{1S} repeats, which are connected by three cytoplasmic loops. The α_{1S} interaction domain, which mediates binding to β_{1a}, is located within the I-II loop (AID, *green*). The critical region, a sequence within the α_{1S} II-III loop with particular importance for skeletal-type EC coupling, is highlighted in *orange*. The constructs were characterized by their ability to target to the plasma membrane-SR junctions (targeting, indicated by the presence of fluorescent foci at or near the cell surface in confocal scans) upon expression in RyR1-KO (dyspedic) and α_{1S} null (dysgenic) myotubes, their ability to support electrically evoked contraction (*contr.*) in dysgenic myotubes, and by the presence of L-type Ca^{2+} currents (I_{Ca}). *Bars*, 5 μm; *n.d.*, not determined.

between residues 726 and 727, and additionally observed that constructs with this insertion displayed junctional targeting in dyspedic myotubes (Fig. 1*d*). We did not test insertions further downstream in the II-III loop because the previous work had shown that signaling interactions with RyR1 were ablated by insertions either between residues 760 and 761, or between residues 785 and 786 (33). In the III-IV loop, we found that insertion at a point near the middle (between residues 1096 and 1097) abolished targeting in both dyspedic and dysgenic myotubes and also eliminated EC coupling (Fig. 1*e*). Given the relatively short length of the III-IV loop (53 residues), we did not test other insertion sites. Based on the results illustrated in Fig. 1, the N terminus, the I-II loop downstream of the AID, and the II-III loop at the beginning of the domain critical for EC coupling were identified as potential sites for double labeling of α_{1S}.

Previous work had shown that attachment of either a CFP-YFP tandem (25), or the biotin acceptor domain (26), to a C-terminally truncated α_{1S} (at residue 1667) did not interfere with function after expression in dysgenic myotubes, and we found similar results for truncation and attachment of YPet at residue 1666 (data not shown). Additionally, we observed that constructs C-terminally tagged with YPet at residue 1666 and N-terminally tagged with CyPet (CyPet-α_{1S}1666-YPet) produced co-localized cyan and yellow puncta after expression in dysgenic myotubes (Fig. 2*a*, *upper row*). Co-localized puncta were also observed after expression of CyPet-α_{1S}1666-YPet in dyspedic myotubes, but this was superimposed on a substantial background of diffuse yellow fluorescence (Fig. 2*a*, *bottom row*). Because post-translational cleavage of full-length α_{1S} (1873 residues) has been reported to occur at residue 1664 (34), this diffuse yellow fluorescence could have been a consequence of the proteolytic liberation of YPet from a fraction of the CyPet-α_{1S}1666-YPet molecules. Thus, we tested the construct CyPet-α_{1S}1636-YPet in which YPet had been attached to the C terminus truncated at residue 1636, upstream of the putative cleavage site. This construct produced co-localized cyan and yellow foci in both dysgenic and dyspedic myotubes (Fig. 2*b*). On the basis of these results, all the C-terminally tagged α_{1S} constructs used for the FRET measurements in this study were truncated at residue 1636. All other α_{1S} constructs did not have this truncation and their sequence ended at residue 1860 (25).

Doubly Labeled α_{1S} Constructs—On the basis of the results illustrated in Figs. 1 and 2, there were potentially six constructs of α_{1S} that could be doubly tagged; these are illustrated in Fig. 3,

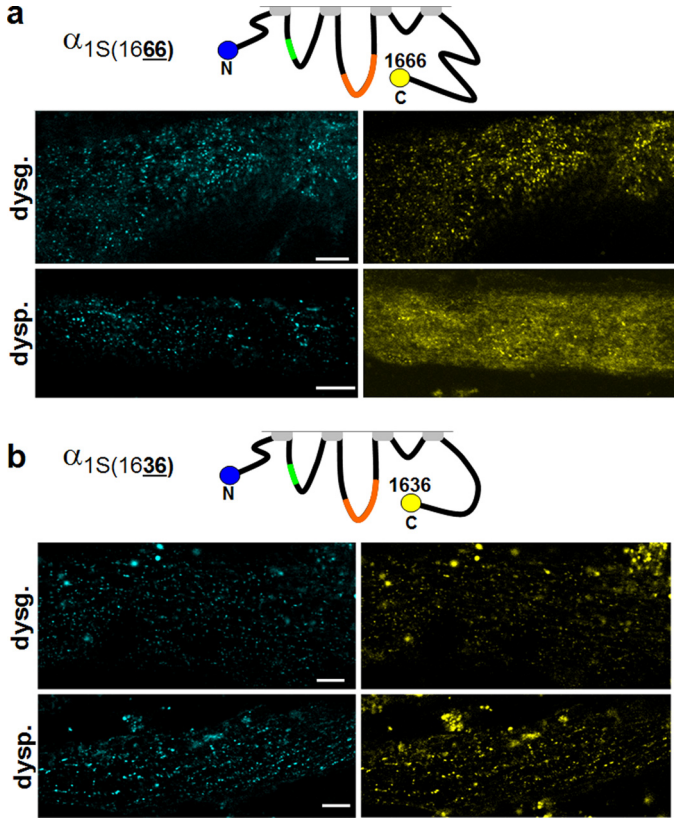

FIGURE 2. **Removal of the distal half of the α_{1S} C terminus preserves α_{1S} function and prevents partial loss of C-terminally attached fluorescent protein in dyspedic myotubes.** Co-localized *cyan* and *yellow* puncta were observed in dysgenic myotubes after expression of α_{1S} that was N-terminally tagged with CyPet and C-terminally tagged with YPet at residue 1666 (*a*). However, when this construct was expressed in dyspedic myotubes, there was a substantial amount of diffuse *yellow* fluorescence, in addition to co-localized *yellow* and *cyan* puncta. The diffuse *yellow* fluorescence was eliminated when the YPet tag was attached to a further truncated C terminus at residue 1636, leaving only co-localized *cyan*/*yellow* puncta in both dysgenic (*dysg.*) and dyspedic (*dysp.*) myotubes (*b*). *Bars*, 5 μm.

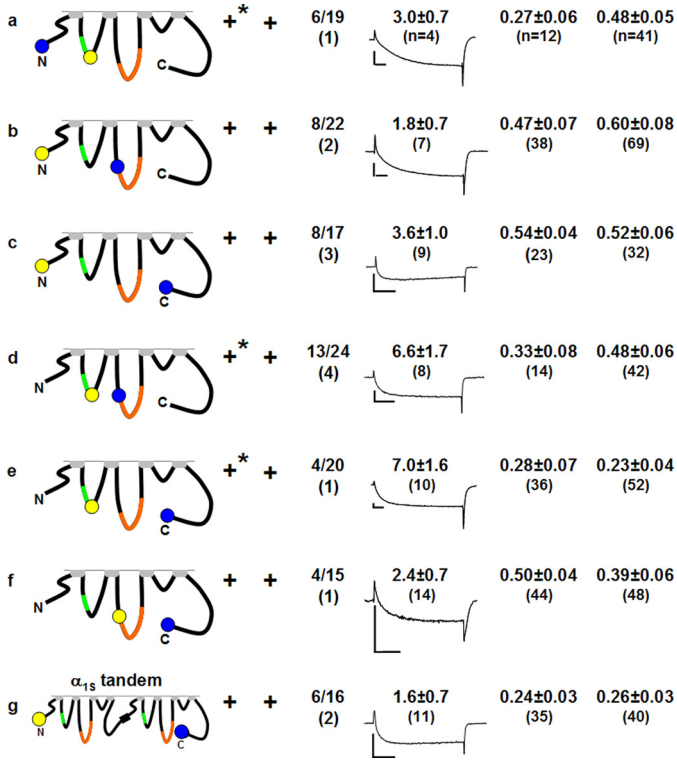

FIGURE 3. **Functional properties and degrees of intramolecular FRET for doubly tagged α_{1S} expressed in dyspedic (*dysp.*) or dysgenic (*dysg.*) myotubes.** All constructs were able to target to the myotube surface, indicated by the presence of discrete fluorescent foci (not shown). In addition to fluorescent puncta, the subunits tagged within the I-II loop (*a*, *d*, and *e*), also displayed a diffuse to reticular intracellular fluorescence when expressed in dyspedic myotubes (indicated by *asterisks* in the targeting column). Only fluorescent puncta were used for analysis. The column lists the fraction of cells that contracted (*contr.*) upon electrical stimulation (indicated as the number of responding cells over the number of cells tested) with the number of spontaneously contracting cells (*spont.*) indicated in *parentheses*. For each of the constructs, the average current density (pA/pF ± S.D.) is shown together with a representative current trace for a test potential of +30 (*b*, *d*, *e*, and *g*) or +40 mV (*a*, *c*, and *f*), with calibration bars corresponding to 2 nA and 50 ms. The quotient I_Y^*/I_C is a measure of the degree of energy transfer from CyPet to YPet (see text for details).

a–f. Surprisingly, all six of the doubly tagged constructs produced, in both dyspedic and dysgenic myotubes, co-localized cyan and yellow foci near/at the cell surface, indicative of successful targeting. In addition to these punctate foci, there was a low level of diffuse/reticular fluorescence in dyspedic myotubes after expression of the three constructs labeled with YPet at position 406 of the I-II loop (*asterisks*, Fig. 3, *a*, *d*, and *e*). For these constructs, a corresponding diffuse/reticular distribution was also observed for the cyan fluorescence, which differs from dyspedic myotubes expressing CyPet-α_{1S}1666-YPet, in which diffuse fluorescence was observed only for the C-terminal tag (Fig. 2*a*) and could be attributed to the freeing of YPet by proteolytic cleavage. Areas of colocalized cyan and yellow fluorescence that were diffuse/reticular were omitted from the analysis of FRET (see "Experimental Procedures"). In addition to the constructs in which two tags were introduced into a single α_{1S}, we also expressed an α_{1S}-α_{1S} tandem labeled on the N terminus with YPet and on the C terminus with CyPet (YPet-α_{1S}-α_{1S}-CyPet). As well as displaying junctional targeting, all of the constructs illustrated in Fig. 3 were able to restore L-type Ca^{2+} current and electrically evoked contractions in dysgenic myotubes, although the fraction of contracting cells was lower than reported for α_{1S} constructs tagged only on the C terminus (33). Based on the previous work in which both electrically evoked contractions and whole-cell Ca^{2+} transients were measured (*cf.* Table 2 of Ref. 33), this indicates that these doubly labeled constructs restored excitation-contraction coupling of reduced efficiency, with the result that the amount of released Ca^{2+} was subthreshold for movement in a significant fraction of the expressing myotubes. Thus, all cells in which the doubly tagged constructs produced discrete fluorescent foci were analyzed for FRET.

The Presence of RyR1 Alters FRET between α_{1S} Cytoplasmic Domains—Both functional and structural evidence strongly support the idea that α_{1S} and RyR1 are linked to one another either directly or via intervening proteins. On first principles, one would expect that these functional and structural interactions would involve cytoplasmic domains of α_{1S}. Thus, as already stated, the main goal of the current work was to test whether the presence of RyR1 causes spatial reorganization of the cytoplasmic domains as indicated by altered FRET between fluorescent probes attached to these domains. For this, we calculated the FRET index I_Y^*/I_C for each of the doubly tagged

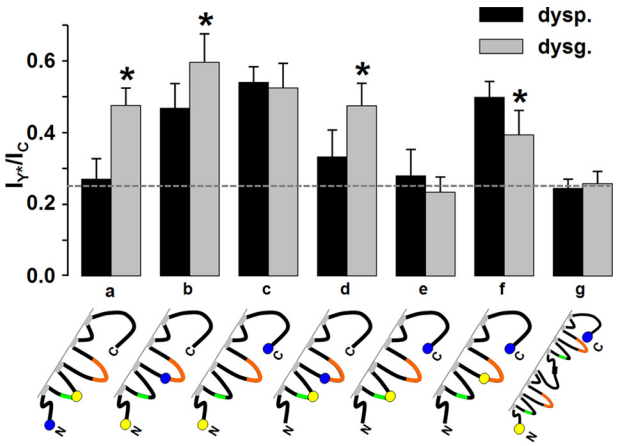

FIGURE 4. **Comparison of the I_Y^*/I_C FRET ratios in the absence (dyspedic) and presence (dysgenic) of RyR1.** *Error bars* indicate S.D., and *asterisks* indicate constructs for which there was a significant ($p < 0.001$) difference in the I_Y^*/I_C ratio between dyspedic (*dysp.*) and dysgenic (*dysg.*) myotubes. Note that the presence of RyR1 increased FRET between the N terminus and both the I-II loop (*a*) and II-III loop (*b*), as well as between the I-II and II-III loops (*d*); the presence of RyR1 decreased FRET between the II-III loop and C terminus (*f*) and had no significant effect on FRET between the N and C termini (*c*). There was no significant FRET between the I-II loop and C terminus in either dyspedic or dysgenic myotubes (*e*). The value of the I_Y^*/I_C ratio in the absence of FRET (0.25, *horizontal dashed line*) was determined as the mean of the I_Y^*/I_C quotients determined for the α_{1S} tandem in dyspedic and dysgenic myotubes (*g*).

constructs both in dyspedic myotubes, where RyR1 is absent, and in dysgenic myotubes where RyR1 is present (Fig. 3). To determine the value of I_Y^*/I_C that corresponds to the absence of FRET, we used the construct YPet-α_{1S}-α_{1S}-CyPet, on the assumption that the N- and C termini of adjacent DHPRs would be separated by too great a distance to support FRET. If this is correct, then the I_Y^*/I_C ratios calculated for the α_{1S} tandem, which were 0.24 ± 0.03 ($n = 35$) and 0.26 ± 0.03 ($n = 40$) for dyspedic and dysgenic myotubes, respectively, should correspond to the absence of FRET for a 1:1 CyPet-YPet stoichiometry. As an experimental test for the absence of FRET, we applied the method of acceptor photobleaching to YPet-α_{1S}-α_{1S}-CyPet expressed in dysgenic myotubes (25). The intensity of CyPet emission (excitation at 440 nm) was the same before and after the photobleaching of YPet by full-power excitation at 515 nm, which supports the assumption that FRET does not occur between the N terminus of the first α_{1S} in the tandem and the C terminus of the second α_{1S}, and that $I_Y^*/I_C \approx 0.25$ represents the absence of FRET.

Fig. 4 presents a graphical comparison of the I_Y^*/I_C values, illustrates how these values depend on the cytoplasmic locations of the donor and acceptor fluorophores, and how they depend on the absence or presence of RyR1. The major results are as follows. First, there was substantial FRET between the N terminus and C terminus (residue 1636), and this did not differ between dyspedic and dysgenic myotubes (Fig. 4*c*). Thus, the presence of RyR1 did not appear to alter the spatial disposition of the N and C termini with respect to one another and they can thus be considered as "anchor points" to which reorientation of other cytoplasmic domains can be related. Second, there is no detectable FRET between the I-II loop (residue 406) and C terminus in either dyspedic or dysgenic myotubes (Fig. 4*e*) in that the I_Y^*/I_C values differed little from those of YPet-α_{1S}-α_{1S}-CyPet (indicated by the *dashed*, *horizontal line*). Third, RyR1 caused the emergence of FRET between the I-II loop and N terminus (Fig. 4*a*) and caused increased FRET between the II-III loop and N terminus (Fig. 4*b*). Fourth, RyR1 caused increased FRET between the I-II and II-III loops (Fig. 4*d*) and decreased FRET between the II-III loop and C terminus (Fig. 4*f*). Overall, these results suggest that the presence of RyR1 causes an appreciable rearrangement of the α_{1S} cytoplasmic domains.

DISCUSSION

In this work, we have described measurements of FRET on intact muscle expressing α_{1S} constructs in which the fluorescent proteins CyPet and YPet were attached to pairs of cytoplasmic domains. We found that junctional targeting, L-type Ca^{2+} current, and EC coupling were all preserved for doubly labeled constructs with the fluorescent proteins attached at the N terminus, I-II loop (residue 406, 33 residues downstream of the AID), II-III loop at residue 726 (*i.e.* within the domain that spans residues 720–765 and is critical for EC coupling), and the C terminus truncated at residue 1636 (Figs. 1–3). When these constructs were expressed in dyspedic myotubes, which lack RyR1, appreciable FRET occurred between the N and C termini, and from the II-III loop to the N terminus, the C terminus, and (to a lesser extent) the I-II loop (Fig. 4). After expression in dysgenic myotubes, in which RyR1 is present, FRET from the N to C terminus was unchanged, from the II-III loop was increased to the N terminus and decreased to the C terminus; for the I-II loop, FRET became measureable to the N terminus and increased to the II-III loop (Fig. 4). Thus, the presence of RyR1 appeared to cause a widespread rearrangement of the cytoplasmic domains of α_{1S}.

Although the changes in FRET are strongly suggestive that the presence of RyR1 causes a reorientation of the α_{1S} cytoplasmic domains, a more specific interpretation in terms of interdomain distances depends upon a number of assumptions that are difficult to test directly. For example, FRET depends not only on distance but also on the donor:acceptor ratio (CyPet:YPet), which we have assumed to be 1:1 for our constructs. However, the "effective" stoichiometry depends upon the extent of maturation (35) of each of the fluorophores and on their local environment (*e.g.* dielectric constant), which could be differentially affected by the presence or absence of RyR1 and thus affect measured FRET. The presence of RyR1 could also alter FRET by affecting the orientation of the donor and acceptor dipoles with respect to one another (36). In addition to these "generic" concerns, which apply to most studies employing FRET, an issue of specific importance for our studies is the extent to which intermolecular FRET, between neighboring DHPRs, might have contributed to the measured FRET values. It seems likely that the FRET measured in the absence of RyR1 was only intramolecular because DHPRs appear to be randomly oriented in dyspedic myotubes (37). In the presence of RyR1, however, the ordered array of DHPR tetrads (37, 38) could have resulted in an additional, intermolecular component that would have increased total FRET. In principle, this might account for the RyR1-associated increase in FRET between the I-II loop and both the N terminus (Fig. 4*a*) and II-III loop (Fig.

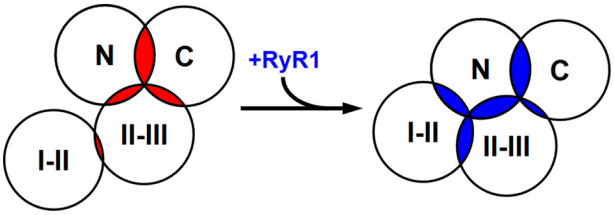

FIGURE 5. **Model of how spatial reorientations of cytoplasmic α_{1S} domains caused by association with RyR1 could account for the observed changes in I_Y^*/I_C.** Shown is a potential arrangement of α_{1S} cytoplasmic domains, viewed from the intracellular side, in the absence (*left*) and presence (*right*) of RyR1. The circles are ~50 Å in radius and the extent of overlap correlates with the extent of FRET (I_Y^*/I_C, Fig. 3) in the absence (*red*) or presence (*blue*) of RyR1 (see text for additional details).

4*b*). Relevant to this issue, earlier experiments examined the spatial interrelationships of β_{1a} subunits in DHPR tetrad arrays by analyzing constructs expressed in α_1 null myotubes. These experiments failed to detect either intermolecular FRET (39) or bimolecular fluorescence complementation (40) between β_{1a} subunits in adjacent DHPRs. Thus, it was suggested that the adjacent β_{1a} subunits were separated from one another by >10 nm (see Fig. 8 in Ref. 40). If this suggested arrangement is correct, then the I-II loops of α_{1S} also would likely be positioned at a distance >10 nm from the α_{1S} cytoplasmic domains of adjacent DHPRs.

Under the assumption that the FRET we measured was produced intramolecularly and is an indication of proximity, our results can be summarized by the diagram in Fig. 5, which represents a cytoplasmic view of α_{1S}. Because the practical limit for measurable FRET is a donor-acceptor distance of ~100 Å (36), the diagram illustrates each of the labeled domains surrounded by an ~50 Å circle and the extent of FRET between any two domains is indicated by the overlap between the circles surrounding those domains. In the absence of RyR1 (overlapping areas indicated in *red*), the N and C termini are close enough to one another to produce an I_Y^*/I_C ratio of 0.54, and, to a slightly lesser degree, the II-III loop is close to both the N and C terminus (I_Y^*/I_C ratios of 0.47 and 0.50, respectively). There is less proximity between the I-II and II-III loops ($I_Y^*/I_C = 0.33$, where 0.25 corresponds to the absence of FRET), and the I-II loop is sufficiently far from both the N and C terminus that there was no detectable FRET. The presence of RyR1 causes a significant rearrangement of both the I-II and II-III loops (Fig. 5, overlapping areas indicated in *blue*). In particular, the II-III loop appears to move away from the C terminus (I_Y^*/I_C decreases to 0.39) and toward the N terminus (I_Y^*/I_C increases to 0.60), and the I-II loop moves toward both the II-III loop and the N terminus (I_Y^*/I_C increases to 0.48 with respect to both). Thus, the overall consequence is that the cytoplasmic domains appear to assume a more compact arrangement when RyR1 is present.

Obviously, Fig. 5 presents an extremely simplified view of the cytoplasmic domains because each of them spans many residues (N terminus, residues 1–51; I-II loop, residues 335–432; II-III loop, residues 662–799; full-length C terminus, residues 1382–1873). Virtually nothing is known about the folding of these domains, but their dimensions would be substantial even if they were folded as compact globular structures (diameters from ~20 to ~50 Å). Thus, one would expect that the interdomain distances inferred from FRET would be strongly dependent on the sites of placement of the donor and acceptor fluorophores. Nonetheless, it seems useful to relate the interdomain relationships inferred from FRET with the results of previous studies bearing on these domains and their possible interactions with other junctional proteins.

It remains unknown whether, *in vivo*, the DHPR and RyR1 contact one another directly, or indirectly via intervening proteins. However, the evidence is compelling that there are structural (5, 6) and functional (7, 8) interactions linking the two. Thus, independent of whether the contacts are direct or indirect, it is valuable to compare our results on RyR1-dependent rearrangements of DHPR cytoplasmic domains with previous work on structural/functional links between the DHPR and RyR1. From this work, it seems unlikely that the N terminus, the smallest domain, interacts structurally or functionally with RyR1 because removal of ~70% (residues 2–37) has essentially no effect on function (41). In the case of the C terminus, the largest domain, it has been reported that residues 1393–1527 bind to a segment of RyR1 *in vitro* (24). However, it is unclear whether such binding to RyR1 also occurs *in vivo*. Specifically, this C-terminal segment is highly conserved in α_{1C}, which appears not bind to RyR1 *in vivo* because tetrads are not observed after expression of α_{1C} in dysgenic myotubes (13). A second role that has been described for the C terminus is in targeting. In particular, C-terminal residues 1607–1661 (42) have been reported to be important for the targeting of α_{1S} to the junctional membrane, and the mutation V1642D in this region was reported to impair targeting (43). However, we found that targeting of α_{1S} could still occur when a fluorescent protein was attached to the C terminus truncated at 1636. Certainly, some targeting can occur in constructs entirely lacking this region because some restoration of EC coupling, which depends on junctional targeting, was reported to occur for α_{1S} truncated at residue 1542 (43). In any event, it seems unlikely that junctional targeting is a result of the binding of DHPR cytoplasmic domains to RyR1, because α_{1S} targets to junctions in muscle cells null for RyR1 (44). The idea that neither the C terminus (proximal to residue 1636) nor the N terminus bind to RyR1 appears to be consistent with our observation that FRET between the N and C terminus (residue 1636) was not affected by the presence or absence of RyR1 (Fig. 4*c*).

Based on a number of studies, it is clear that the functional and structural interactions between the DHPR and RyR1 depend on both the II-III loop of α_{1S} and the β_{1a} auxiliary subunit. For example, expression of chimeras containing various combinations of sequence from α_{1S}, α_{1C}, and α_{1M} has shown that the presence of α_{1S} sequence in the II-III loop (roughly, residues 720–765) is required both for skeletal-type EC coupling (16, 45) and for the formation of DHPR tetrads (13). Similarly, expression of different β isoforms in β_1 null myotubes from mouse (46) and zebrafish (21) has shown that only β_{1a} is able to restore full, skeletal type EC coupling. A possibility raised by these data is that the II-III loop and/or β_{1a} bind to RyR1. Indeed, *in vitro* binding of II-III loop residues 720–765 to RyR1 residues 1837–2168 (47) and of β_{1a} to RyR1 (48) have both been reported. As for other instances of *in vitro* binding of DHPR domains to RyR1, however, it is uncertain that this binding occurs *in vivo*. In particular, even though some α_{1S} is pres-

ent in the membrane of β_1 null zebrafish muscle cells, it is not arrayed as tetrads (19), indicating that α_{1S} does not bind to RyR1 in the absence of the β subunit. Conversely, in α_{1S} null myotubes, fluorescently tagged β_{1a} does not bind to RyR1 (18) and is freely diffusible (39). Thus, it appears that even though there must be protein-protein contacts linking the DHPR and RyR1, identifying these contacts may not be feasible using isolated components of the DHPR complex. For example, one could imagine that a high affinity interaction required the simultaneous binding of β_{1a} and the α_{1S} II-III loop to RyR1 domains, which form a single binding pocket in three dimensions. If so, it might explain why the FRET results suggest a decreased separation between the I-II loop (to which β_{1a} is attached) and the II-III loop when RyR1 is present (Fig. 4). Interestingly, the larger separation between the I-II and II-III loops in the absence of RyR1 may be represented in the structure of the isolated DHPR determined by electron cryo-microscopy (49), in which β_{1a} appears to be deflected laterally with respect to α_{1S}.

The approach we have employed here, of measuring FRET for doubly tagged α_{1S} constructs expressed in myotubes, is useful because it provides spatial information about functional DHPRs in plasma membrane/SR junctions. However, as already discussed above, this information is necessarily somewhat imprecise. Nonetheless, this information provides obvious directions for future experiments. For example, it will be important to determine whether the interdomain FRET changes in response to depolarization and whether such changes correlate with activation of Ca^{2+} release via RyR1. Similarly, it will be of interest to determine whether these FRET signals are altered by application of pharmacological agents (*e.g.* ryanodine, dihydropyridines) or by mutations of α_{1S} and RyR1 that are associated with human muscular disorders.

Acknowledgment—We are indebted to Dr. P. S. Daugherty who provided us with the CyPet and Ypet expression plasmids.

REFERENCES

1. Franzini-Armstrong, C. (1970) Studies of the triad. I. Structure of the junction in frog twitch fibers. *J. Cell Biol.* **47,** 488–499
2. Schneider, M. F., and Chandler, W. K. (1973) Voltage dependent charge movement of skeletal muscle: A possible step in excitation–contraction coupling. *Nature* **242,** 244–246
3. Tanabe, T., Beam, K. G., Powell, J. A., and Numa, S. (1988) Restoration of excitation-contraction coupling and slow calcium current in dysgenic muscle by dihydropyridine receptor complementary DNA. *Nature* **336,** 134–139
4. Inui, M., Saito, A., and Fleischer, S. (1987) Purification of the ryanodine receptor and identity with feet structures of junctional terminal cisternae of sarcoplasmic reticulum from fast skeletal muscle. *J. Biol. Chem.* **262,** 1740–1747
5. Block, B. A., Imagawa, T., Campbell, K. P., and Franzini-Armstrong, C. (1988) Structural evidence for direct interaction between the molecular components of the transverse tubule/sarcoplasmic reticulum junction in skeletal muscle. *J. Cell Biol.* **107,** 2587–2600
6. Paolini, C., Fessenden, J. D., Pessah, I. N., and Franzini-Armstrong, C. (2004) Evidence for conformational coupling between two calcium channels. *Proc. Natl. Acad. Sci. U.S.A.* **101,** 12748–12752
7. Armstrong, C. M., Bezanilla, F. M., and Horowicz, P. (1972) Twitches in the presence of ethylene glycol bis(-aminoethyl ether)-*N,N′*-tetracetic acid. *Biochim. Biophys. Acta* **267,** 605–608
8. Dirksen, R. T. (2002) Bi-directional coupling between dihydropyridine receptors and ryanodine receptors. *Front. Biosci.* **7,** d659–670
9. Protasi, F., Paolini, C., Nakai, J., Beam, K. G., Franzini-Armstrong, C., and Allen, P. D. (2002) Multiple regions of RyR1 mediate functional and structural interactions with α(1S)-dihydropyridine receptors in skeletal muscle. *Biophys. J.* **83,** 3230–3244
10. Sheridan, D. C., Takekura, H., Franzini-Armstrong, C., Beam, K. G., Allen, P. D., and Perez, C. F. (2006) Bidirectional signaling between calcium channels of skeletal muscle requires multiple direct and indirect interactions. *Proc. Natl. Acad. Sci. U.S.A.* **103,** 19760–19765
11. Tanabe, T., Takeshima, H., Mikami, A., Flockerzi, V., Takahashi, H., Kangawa, K., Kojima, M., Matsuo, H., Hirose, T., and Numa, S. (1987) Primary structure of the receptor for calcium channel blockers from skeletal muscle. *Nature* **328,** 313–318
12. Pragnell, M., De Waard, M., Mori, Y., Tanabe, T., Snutch, T. P., and Campbell, K. P. (1994) Calcium channel β-subunit binds to a conserved motif in the I-II cytoplasmic linker of the α1-subunit. *Nature* **368,** 67–70
13. Takekura, H., Paolini, C., Franzini-Armstrong, C., Kugler, G., Grabner, M., and Flucher, B. E. (2004) Differential contribution of skeletal and cardiac II-III loop sequences to the assembly of dihydropyridine-receptor arrays in skeletal muscle. *Mol. Biol. Cell* **15,** 5408–5419
14. Tanabe, T., Beam, K. G., Adams, B. A., Niidome, T., and Numa, S. (1990) Regions of the skeletal muscle dihydropyridine receptor critical for excitation-contraction coupling. *Nature* **346,** 567–569
15. Lu, X., Xu, L., and Meissner, G. (1994) Activation of the skeletal muscle calcium release channel by a cytoplasmic loop of the dihydropyridine receptor. *J. Biol. Chem.* **269,** 6511–6516
16. Nakai, J., Tanabe, T., Konno, T., Adams, B., Beam, K. G. (1998) Localization in the II-III loop of the dihydropyridine receptor of a sequence critical for excitation-contraction coupling. *J. Biol. Chem.* **273,** 24983–24986
17. Grabner, M., Dirksen, R. T., Suda, N., and Beam, K. G. (1999) The II-III loop of the skeletal muscle dihydropyridine receptor is responsible for the bi-directional coupling with the ryanodine receptor. *J. Biol. Chem.* **274,** 21913–21919
18. Neuhuber, B., Gerster, U., Döring, F., Glossmann, H., Tanabe, T., and Flucher, B. E. (1998) Association of calcium channel α1S and β1a subunits is required for the targeting of β1a but not of α1S into skeletal muscle triads. *Proc. Natl. Acad. Sci. U.S.A.* **95,** 5015–5020
19. Schredelseker, J., Di Biase, V., Obermair, G. J., Felder, E. T., Flucher, B. E., Franzini-Armstrong, C., and Grabner, M. (2005) The β1a subunit is essential for the assembly of dihydropyridine-receptor arrays in skeletal muscle. *Proc. Natl. Acad. Sci. U.S.A.* **102,** 17219–17224
20. Coronado, R., Ahern, C. A., Sheridan, D. C., Cheng, W., Carbonneau, L., and Bhattacharya, D. (2004) Functional equivalence of dihydropyridine receptor alpha1S and beta1a subunits in triggering excitation-contraction coupling in skeletal muscle. *Biol. Res.* **37,** 565–575
21. Schredelseker, J., Dayal, A., Schwerte, T., Franzini-Armstrong, C., and Grabner, M. (2009) Proper restoration of excitation-contraction coupling in the dihydropyridine receptor beta1-null zebrafish relaxed is an exclusive function of the beta1a subunit. *J. Biol. Chem.* **284,** 1242–1251
22. Weiss, R. G., O'Connell, K. M., Flucher, B. E., Allen, P. D., Grabner, M., and Dirksen, R. T. (2004) Functional analysis of the R1086H malignant hyperthermia mutation in the DHPR reveals an unexpected influence of the III-IV loop on skeletal muscle EC coupling. *Am. J. Physiol. Cell Physiol.* **287,** C1094-C1102
23. Bannister, R. A., Grabner, M., and Beam, K. G. (2008) The α(1S) III-IV loop influences 1,4-dihydropyridine receptor gating but is not directly involved in excitation-contraction coupling interactions with the type 1 ryanodine receptor. *J. Biol. Chem.* **283,** 23217–23223
24. Sencer, S., Papineni, R. V., Halling, D. B., Pate, P., Krol, J., Zhang, J. Z., and Hamilton, S. L. (2001) Coupling of RYR1 and L-type calcium channels via calmodulin binding domains. *J. Biol. Chem.* **276,** 38237–38241
25. Papadopoulos, S., Leuranguer, V., Bannister, R. A., and Beam, K. G. (2004) Mapping sites of potential proximity between the dihydropyridine receptor and RyR1 in muscle using a cyan fluorescent protein-yellow fluorescent protein tandem as a fluorescence resonance energy transfer probe. *J. Biol. Chem.* **279,** 44046–44056

26. Lorenzon, N. M., and Beam, K. G. (2007) Accessibility of targeted DHPR sites to streptavidin and functional effects of binding on EC coupling. *J. Gen. Physiol.* **130,** 379–388
27. Nguyen, A. W., and Daugherty, P. S. (2005) Evolutionary optimization of fluorescent proteins for intracellular FRET. *Nat. Biotechnol.* **23,** 355–360
28. Knudson C. M., Chaudhari, N., Sharp, A. H., Powell, J. A., Beam, K. G., and Campbell, K. P. (1989) Specific absence of the α1 subunit of the dihydropyridine receptor in mice with muscular dysgenesis. *J. Biol. Chem.* **264,** 1345–1348
29. Buck, E. D., Nguyen, H. T., Pessah, I. N., and Allen, P. D. (1997) Dyspedic mouse skeletal muscle expresses major elements of the triadic junction but lacks detectable ryanodine receptor protein and function. *J. Biol. Chem.* **272,** 7360–7367
30. Beam, K. G., and Franzini-Armstrong, C. (1997) Functional and structural approaches to the study of excitation-contraction coupling. *Methods Cell Biol.* **52,** 283–306
31. Hamill, O. P., Marty, A., Neher, E., Sakmann, B., and Sigworth, F. J. (1981) Improved patch-clamp techniques for high-resolution current recording from cells and cell-free membrane patches. *Pflugers Arch.* **391,** 85–100
32. De Waard, M., Witcher, D. R., Pragnell, M., Liu, H., and Campbell, K. P. (1995) Properties of the α1-β anchoring site in voltage-dependent Ca^{2+} channels. *J. Biol. Chem.* **270,** 12056–12064
33. Bannister, R. A., Papadopoulos, S., Haarmann, C. S., and Beam, K. G. (2009) Effects of inserting fluorescent proteins into the alpha1S II-III loop: insights into excitation-contraction coupling. *J. Gen. Physiol.* **134,** 35–51
34. Hulme, J. T., Konoki, K., Lin, T. W., Gritsenko, M. A., Camp, D. G., 2nd, Bigelow, D. J., and Catterall, W. A. (2005) Sites of proteolytic processing and noncovalent association of the distal C-terminal domain of $Ca_V1.1$ channels in skeletal muscle. *Proc. Natl. Acad. Sci. U.S.A.* **102,** 5274–5279
35. Tsien, R. Y. (1998) The green fluorescent protein. *Annu. Rev. Biochem.* **67,** 509–544
36. dos Remedios, C. G., and Moens, P. D. (1995) Fluorescence resonance energy transfer spectroscopy is a reliable "ruler" for measuring structural changes in proteins. Dispelling the problem of the unknown orientation factor. *J. Struct. Biol.* **115,** 175–185
37. Protasi, F., Franzini-Armstrong, C., and Allen, P. D. (1998) Role of ryanodine receptors in the assembly of calcium release units in skeletal muscle. *J. Cell Biol.* **140,** 831–842
38. Sun, X. H., Protasi, F., Takahashi, M., Takeshima, H., Ferguson, D. G., and Franzini-Armstrong, C. (1995) Molecular architecture of membranes involved in excitation-contraction coupling of cardiac muscle. *J. Cell Biol.* **129,** 659–671
39. Leuranguer, V., Papadopoulos, S., and Beam, K. G. (2006) Organization of calcium channel β1a subunits in triad junctions in skeletal muscle. *J. Biol. Chem.* **281,** 3521–3527
40. Sheridan, D. C., Moua, O., Lorenzon, N. M., and Beam, K. G. (2012) Bimolecular fluorescence complementation and targeted biotinylation provide insight into the topology of the skeletal muscle Ca^{2+} channel β1a subunit. *Channels* **6,** 26–40
41. Bannister, R. A., and Beam, K. G. (2005) The α1S N-terminus is not essential for bi-directional coupling with RyR1. *Biochem. Biophys. Res. Commun.* **336,** 134–141
42. Flucher, B. E., Kasielke, N., and Grabner, M. (2000) The triad targeting signal of the skeletal muscle calcium channel is localized in the COOH terminus of the α(1S) subunit. *J. Cell Biol.* **151,** 467–478
43. Proenza, C., Wilkens, C., Lorenzon, N. M., and Beam, K. G. (2000) A carboxyl-terminal region important for the expression and targeting of the skeletal muscle dihydropyridine receptor. *J. Biol. Chem.* **275,** 23169–23174
44. Takekura, H., and Franzini-Armstrong, C. (1999) Correct targeting of dihydropyridine receptors and triadin in dyspedic mouse skeletal muscle *in vivo*. *Dev. Dyn.* **214,** 372–380
45. Kugler, G., Weiss, R. G., Flucher, B. E., and Grabner, M. (2004) Structural requirements of the dihydropyridine receptor α1S II-III loop for skeletal-type excitation-contraction coupling. *J. Biol. Chem.* **279,** 4721–4728
46. Beurg, M., Sukhareva, M., Ahern, C. A., Conklin, M. W., Perez-Reyes, E., Powers, P. A., Gregg, R. G., and Coronado, R. (1999) Differential regulation of skeletal muscle L-type Ca^{2+} current and excitation-contraction coupling by the dihydropyridine receptor β subunit. *Biophys. J.* **76,** 1744–1756
47. Proenza, C., O'Brien, J., Nakai, J., Mukherjee, S., Allen, P. D., and Beam, K. G. (2002) Identification of a region of RyR1 that participates in allosteric coupling with the α_{1S} ($Ca_V1.1$) II-III loop. *J. Biol. Chem.* **277,** 6530–6535
48. Cheng, W., Altafaj, X., Ronjat, M., and Coronado, R. (2005) Interaction between the dihydropyridine receptor Ca^{2+} channel β-subunit and ryanodine receptor type 1 strengthens excitation-contraction coupling. *Proc. Natl. Acad. Sci. U.S.A.* **102,** 19225–19230
49. Wolf, M., Eberhart, A., Glossmann, H., Striessnig, J., and Grigorieff, N. (2003) Visualization of the domain structure of an L-type Ca^{2+} channel using electron cryo-microscopy. *J. Mol. Biol.* **332,** 171–182